Electrical transport properties of benzene-derived graphite fibers

L. D. Woolf, J. Chin, Y. R. Lin-Liu, and H. Ikezi
GA Technologies, Inc., P.O. Box 85608, San Diego, California 92138
(Received 28 December 1983)

Detailed measurements of the transverse magnetoresistance of a benzene-derived graphite fiber annealed at 3000 °C have been carried out between temperatures of 1.4 and 249 K and in magnetic fields between 30 and 80 000 G. Using a modification of a simple two-band theory due to Noto and Tsuzuku, we have been able to generate a good fit to the magnetoresistance data over the entire magnetic field range studied. Using this model, we find that the mobility varies from 9.8×10^3 $cm^2/V\,sec$ at 249 K to 3.2×10^4 $cm^2/V\,sec$ at 1.4 K, the total carrier density varies from $9.7\times10^{18}/cm^3$ at 249 K to $3\times10^{18}/cm^3$ at 1.4 K, and $|(n_e-n_h)/(n_e+n_h)|$ changes from 0.21 at 249 K to 0.094 at 1.4 K. Various other models have also been employed to estimate carrier densities and mobilities. Using simple theories, we can fit the temperature dependence of the mobility, the carrier density, and the resistivity. We show that changes in the temperature dependence of the resistivity of pyrolytic graphites and benzene-derived graphite fibers annealed at temperatures between ~2500 and 3500 °C can be understood simply by changes in the crystallite size which alter the amount of boundary scattering.

I. INTRODUCTION

Recently, Endo *et al.*[1] and Chieu *et al.*[2] have reported magnetoresistance measurements on highly graphitized benzene-derived fibers (BDF's). These fibers have stimulated considerable interest[1–15] due to their being highly graphitizable, considerably more so than either polyacrylonitrile (PAN) or mesophase pitch-derived fibers. The graphitic structure of the annealed BDF's leads to a positive magnetoresistance whereas most PAN and pitch fibers exhibit negative magnetoresistance. However, the magnetoresistance of the BDF's in high magnetic fields is approximately 1 order of magnitude smaller than that of highly oriented pyrolytic graphite (HOPG).[2] Since the magnetoresistance is a probe of the carrier mobility, this suggests that the carrier mobility in the BDF is significantly reduced from that of HOPG.[2]

Endo *et al.*[2] have performed an extensive study of the magnetic field and angular dependence of the magnetoresistance at 77 K of BDF's annealed at a variety of heat-treatment temperatures. Chieu *et al.*[2] have examined the magnetic field and angular dependence of the high-field magnetoresistance of the BDF at 4.2 K. However, neither study attempted to derive carrier mobilities or carrier densities from their data. In addition, neither paper examined the temperature dependence of these transport quantities.

In this paper we show the results of a study of the magnetoresistance of a BDF, heat-treated to 3000 °C, in magnetic fields between 30 G and 80 kG and at temperatures between 1.4 and 249 K. Using various models, we derive carrier densities and carrier mobilities as a function of temperature and discuss their implications.

II. EXPERIMENTAL DETAILS

Carbon fibers up to 10 cm long were grown from a mixture of benzene and hydrogen on an iron-powder-catalyzed substrate between 1100 and 1300 °C. Graphitization of the vapor-deposited fibers was done in outgassed graphite crucibles. The crucible and fibers were heated in high-purity argon to 3000 °C with an electrical-resistance furnace and then held at 3000 °C for 3 min. Temperatures were measured with an optical pyrometer which was calibrated against a standard tungsten lamp at 2300 °C and cross-checked against a two-color infrared pyrometer at 3000 °C. Scanning-electron-microscope photomicrographs show the annealed fibers to have a polygonalized cross section that had previously been reported by Koyama *et al.*[6]

A 35-μm-diam fiber was mounted in air and set on a sapphire block to decrease its thermal resistance to the copper heat sink on which the thermometers were mounted. Electrical contact to the sample was made using silver paint to attach four 0.001-in.-diam copper wires. A dc four-terminal method was used with the current having the constant value of 100 μA. Thermal emf's were minimized by nulling them out at each temperature in zero magnetic field. As a check, the magnetoresistance derived using the dc method was compared at various temperatures and magnetic fields with that obtained using a phase-sensitive ac technique and good agreement was always found. The fiber was mounted perpendicular to the applied magnetic field so that the transverse magnetoresistance was probed. Since the fiber morphology has its graphite planes arranged cylindrically like the rings of a tree about the fiber axis,[6] the in-plane electrical conductivity was measured in this experiment. In comparing our data with that taken by other workers on pyrolytic graphites, we implicitly mean to compare our data with their in-plane data.

Measurements were performed in a Janis Supervaritemp Dewar with an 8-T superconducting magnet. The sample was always in contact with either flowing or static helium gas. To monitor the temperature, a calibrated germanium-resistance thermometer, a carbon-

glass—resistance thermometer, and a calibrated silicon-diode thermometer were mounted on the copper heat sink. At each new temperature in zero magnetic field, the carbon-glass thermometer was calibrated using either the germanium thermometer and/or the silicon-diode thermometer. In applied magnetic fields, the temperature was stabilized by using a Linear Research model no. LR-400 four-wire ac resistance bridge to monitor the resistance of the carbon-glass thermometer in conjunction with a Linear Research model no. LR-130 temperature controller which drove a heater mounted on the thermal shield of the sample holder. The temperature (T) stability was better than $\pm 0.01T$.

Data were collected automatically using an IBM Personal Computer in conjunction with a TECMAR model no. 20030 IEEE-488 board. The computer read the sample voltage and the current through the magnet via two Keithley model no. 195 digital multimeters. The data were stored on magnetic disk for later analysis.

III. MAGNETORESISTANCE

Analyses of magnetoresistance data on pyrolytic graphites (PG's) and single-crystal graphite have been carried out by numerous researchers. Klein investigated the galvanomagnetic properties of pyrolytic graphites deposited from methane, heat-treated up to $\sim 3500\,^{\circ}\mathrm{C}$.[16,17] Using a simple two-band (STB) model and assuming that the hole mobility μ_h is equal to the electron mobility μ_e, that the hole carrier density n_h is equal to the electron carrier density n_e, and that $(\bar{\mu}H)^2 \ll 1$, Klein found that

$$\frac{\Delta\rho}{\rho_0} = \bar{\mu}^2 H^2 , \tag{1}$$

or

$$\bar{\mu} = \left[\frac{\Delta\rho}{\rho_0}\right]^{1/2} \frac{1}{H} , \tag{2}$$

where $\bar{\mu} = (\mu_e \mu_h)^{1/2}$, H is the magnetic field, ρ_0 is the zero-magnetic-field resistivity, and $\Delta\rho = \rho(H) - \rho_0$. Klein[16] found that the region over which $\Delta\rho/\rho_0$ obeyed an H^2 dependence decreased as the heat-treatment temperature (and hence degree of graphitization) increased. Values of the mobility were derived using the above expression with the magnetoresistance value at 2500 G. Carrier densities were obtained using

$$\rho = 1/ne\bar{\mu} , \tag{3}$$

so that

$$n = n_e + n_h = \left[e\rho_0 \left[\frac{\Delta\rho}{\rho_0}\right]^{1/2} \frac{1}{H}\right]^{-1} . \tag{4}$$

Klein also analyzed magnetoresistance data taken on a "pyrofiber" annealed at 2800 °C.[16] Taking the angle between the crystallite c axis and the magnetic field direction to be θ, with the current flow always perpendicular to both the crystallite c axis and the magnetic field direction, he estimated the resultant fiber magnetoresistance to be

$$\frac{\Delta\rho}{\rho_0} = \frac{1}{2\pi}\int_0^{2\pi} \left[\frac{\Delta\rho}{\rho_0}\right]_\theta d\theta = \frac{1}{2\pi}\int_0^{2\pi} \left[\frac{\Delta\rho}{\rho_0}\right]_T \cos^2\theta \, d\theta , \tag{5}$$

so

$$\frac{\Delta\rho}{\rho_0} = \frac{1}{2}\left[\frac{\Delta\rho}{\rho_0}\right]_T = \tfrac{1}{2}\bar{\mu}^2 H^2 , \tag{6}$$

where

$$\left[\frac{\Delta\rho}{\rho_0}\right]_T \left[\left[\frac{\Delta\rho}{\rho_0}\right]_\theta\right]$$

is the transverse magnetoresistance obtained from a crystallite whose c axis is aligned parallel (at an angle θ) to the magnetic field direction. The carrier mobility was then calculated using

$$\bar{\mu} = \sqrt{2}\left[\frac{\Delta\rho}{\rho_0}\right]^{1/2} \frac{1}{H} , \tag{7}$$

while the carrier density was derived via Eq. (3).

Soule[18] examined the magnetoresistance of various natural graphite single crystals in considerable detail. He also used Eq. (2) to determine the mobility using values of the magnetoresistance at $H = 3000$ G. Total carrier densities were again derived using Eq. (4) and these values were found to be in good agreement with those calculated using the multicarrier model of McClure.[19]

More recently, Noto and Tsuzuku[20] derived a two-band theory of galvanomagnetic effects in graphite explicitly including the angular dependence of the magnetic field with respect to the graphite c axis. This theory accounted successfully for the angular dependence of the transverse magnetoresistance of iron-melt graphite. The expression they derived for nearly compensated specimens ($n_e \approx n_h$) was

$$\frac{\Delta\rho}{\rho_0} = \frac{\bar{\mu}^2 H^2 \Theta}{1 + [(n_e - n_h)/(n_e + n_h)]^2 \bar{\mu} H^2 \Theta} , \tag{8}$$

where $\Theta = \cos^2\theta + \alpha_3 \sin^2\theta$, θ is the angle between the magnetic field and the graphite c axis (and the current flow is perpendicular to these two directions), α_3 is estimated to be $1/(12.1)^2$, and $\bar{\mu} = \mu_e = \mu_h$ is assumed. Rewriting Eq. (8) as

$$\frac{H^2\Theta}{\Delta\rho/\rho_0} = \frac{1}{\bar{\mu}^2} + \left[\frac{n_e - n_h}{n_e + n_h}\right]^2 H^2\Theta , \tag{9}$$

and plotting the left-hand side versus H^2 results in a straight line. This curve was found to fit the magnetoresistance of kish and pyrolytic graphites in magnetic fields above ~ 5 kG, deviations occurring in lower fields due to minority carrier effects.[20–22]

Finally, Dillon *et al.*[23] have measured the galvanomagnetic properties of highly oriented pyrolytic graphite and compared their results with those derived from natural graphite single crystals. These authors critically analyzed various derivations of the carrier mobility from the magnetoresistance data and concluded that an appropriate measure of the mobility would be Eq. (2), where the

values of the parameters would be taken at $\Delta\rho/\rho_0=1$ so that

$$\bar{\mu}=1/H \ . \tag{10}$$

IV. EXPERIMENTAL RESULTS

Some representative magnetoresistance curves plotted as $\Delta\rho/\rho_0$ versus magnetic field H are displayed in Fig. 1. We also observe the relatively large positive magnetoresistance previously reported for the BDF and note that our data are in quantitative agreement with these previously published reports.[1,2] As expected, the magnitude of the magnetoresistance decreases as the temperature increases, indicating an expected decrease of carrier mobility with increasing temperature.

Chieu *et al.*[2] have reported that at 4.2 K, the BDF exhibits $\Delta\rho/\rho_0 \propto H^2$ at very low fields, followed by a linear field dependence for intermediate-field values. Endo *et al.*,[1] on the other hand, have reported that $\Delta\rho/\rho_0 \propto H^b$, where $b=1.7$ for a BDF heat-treated above 2600 °C at a field below 4 kG at 77 K, and that b decreases gradually with increasing field. To ascertain the behavior of b from our data, we have made sliding least-squares fits of the data to a function of the form $\Delta\rho/\rho_0=aH^b$ and plotted b as a function of H at each of the temperatures examined. Shown in Fig. 2 is a plot of b versus temperature only for magnetic field values of 0 and 30 kG. Our data for b exhibit some scatter in low fields, while at higher fields, the scatter is considerably less. While our data differ significantly from those reported by Soule[18] on single crystals, they are in reasonable agreement with the values cited by Endo *et al.*[1] and Chieu *et al.*[2]

Even though the transverse magnetoresistance data do not precisely obey an H^2 dependence at low fields at all temperatures examined, we will attempt to derive mobility values from the low-field data. Visual best fits to the low-field data plotted as $\Delta\rho/\rho_0$ versus H^2 were made, at each temperature, to Eq. (6), and mobility values were derived using this equation. The temperature dependence of the mobility derived in this manner is plotted in Fig. 3. Interestingly, the qualitative behavior observed here is similar to that observed by Kawamura *et al.*[21] for kish graphite (an iron-melt single crystal), namely a constant

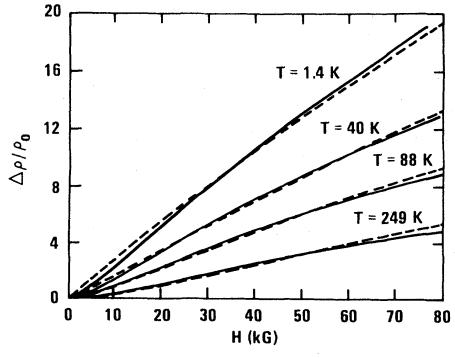

FIG. 1. Magnetoresistance vs magnetic field H for a BDF at a variety of temperatures (dashed curve). Also shown are fits to the data using Eq. (17) (solid line).

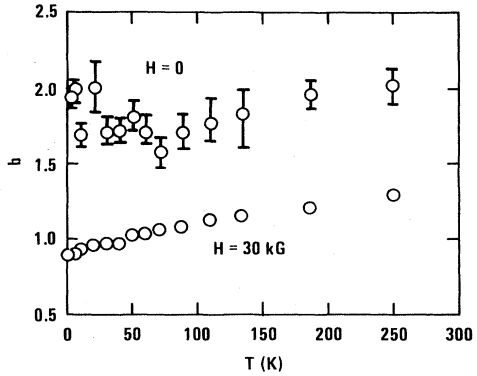

FIG. 2. Exponential dependence of the magnetoresistance power law b vs temperature T for magnetic fields of 0 and 30 kG where $\Delta\rho/\rho_0=aH^b$.

slope between ~110 and 300 K, a slope increasing in magnitude down to ~60 K, and finally a saturation of the mobility at lower temperatures. However, the magnitudes of the slopes (as well as the absolute values of the mobility) differ considerably. Between 120 and 250 K, we find $\bar{\mu}(T)\sim T^{-0.7}$ (compared to $T^{-1.2}$), while between 65 and 115 K, we find $\bar{\mu}(T)\sim T^{-1.3}$ (compared to $T^{-1.6}$). Using these values of the mobility as well as the resistivity values plotted in Fig. 4, the total carrier density shown in Fig. 5 was derived using Eq. (3). However, since this method of analysis has not been generally adopted, we will proceed to discuss three other algorithms for calculating carrier mobilities.

In keeping with the method of analyses employed by both Klein[16] and Soule[18] and suggested by Spain,[24] we have also derived mobility values via Eq. (7) using the value of the resistivity in a field of $H=3000$ G. The temperature dependence of the mobility derived in this manner is also presented in Fig. 3. The mobility is seen to behave in a rather smooth manner and tends to a saturation value below ~20 K. The carrier density derived as stated above is plotted as a function of temperature in Fig. 5. It saturates below ~10 K and exhibits a linear tem-

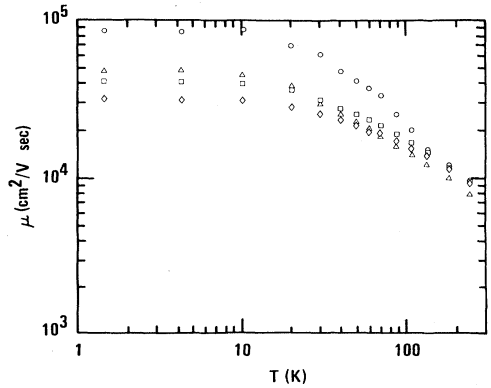

FIG. 3. Mobility μ vs temperature T derived with use of the magnetoresistance data in the low-field limit (circles), from 3000-G data (squares), from data where $\rho(H)/\rho_0=1.5$ (triangles), and from a modified Noto-Tsuzuku theory, Eq. (17) (diamonds).

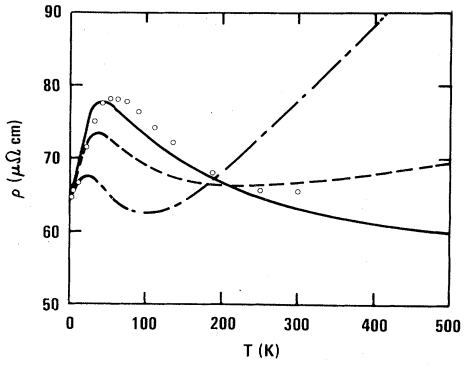

FIG. 4. Resistivity ρ vs temperature T for the BDF (circles). The theoretical resistivity curves were derived with the use of Eq. (3) with n calculated from Eq. (13) with $n(T=0)=3\times10^{18}/\text{cm}^3$ and $E_F=0.0053$ eV and μ calculated from Eq. (19) with parameters $\mu_{BS}=3.3\times10^4$ cm^2/V sec and $\mu_{ph}(T)=(3.4\times10^6)T^{-1.0}$ cm^2/V sec (solid curve); $\mu_{BS}=3.19\times10^4$ cm^2/V sec and $\mu_{ph}(T)=(1\times10^7)T^{-1.2}$ cm^2/V sec (dashed curve); and $\mu_{BS}=3.19\times10^4$ cm^2/V sec and $\mu_{ph}(T)=(8\times10^7)T^{-1.6}$ cm^2/V sec (long-dashed–short-dashed curve).

perature dependence at higher temperatures. We saw no evidence for an increase in the carrier concentration with decreasing temperature in the range below ~15 K, as reported by Klein.[16,17] Using the STB model, Klein[16] has fitted his carrier concentration data derived in the above manner reasonably successfully. The model states that

$$n_h=C_hk_BT\ln[1+\exp(E_0-E_F)/k_BT] \tag{11}$$

and

$$n_e=C_ek_BT\ln[1+\exp(E_F/k_BT)]\ , \tag{12}$$

where E_F denotes the Fermi energy, E_0-E_F is one-half of the band overlap, and C_e and C_h are constants. Assuming that $n_e=n_h$, $C_e=C_h$, and $E_0-E_F=E_F$, i.e., the Fermi energy lies right in the middle of the band overlap, then the total carrier concentration is given by

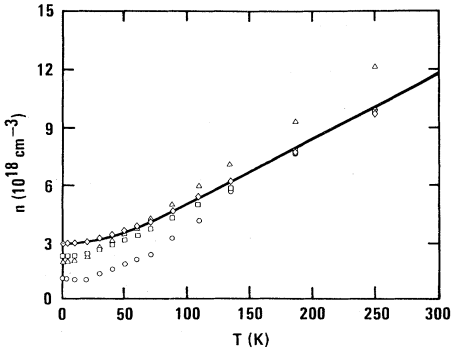

FIG. 5. Total carrier density n vs temperature T derived using the data of Figs. 3 and 4 and Eq. (3). The data were derived from measurements in the low-field limit (circles), from 3000-G data (squares), from data where $\rho(H)/\rho_0=1.5$ (triangles), and Eq. (17) (diamonds). Also displayed is a fit to the data derived from Eq. (17) using Eq. (13) with $n(T=0)=3\times10^{18}/\text{cm}^3$ and $E_F=0.0053$ eV.

$$n=Ck_BT\ln[1+\exp(E_F/k_BT)]\ , \tag{13}$$

where C is a constant. Using Eq. (13), we fit the n-versus-T data of Fig. 5 very well over the entire temperature range. The best-fit parameters derived were $E_F=0.004$ eV, corresponding to a band overlap of 0.008 eV, and $n(T=0)=2.31\times10^{18}/\text{cm}^3$.

We have also employed the method suggested by Dillon *et al.*[23] for deriving carrier mobilities from the magnetoresistance data, i.e., $\bar{\mu}=1/H$ [Eq. (10)]. Previously, we showed that an appropriate modification of Eq. (2) for a fiber's geometry would be Eq. (7). From Eq. (7), the value of $\Delta\rho/\rho_0$ at which $\bar{\mu}=1/H$ is given by $\Delta\rho/\rho_0=0.5$ or $\rho(H)=1.5\rho_0$. Using this procedure, we calculated $\bar{\mu}$ and its resultant temperature dependence as shown in Fig. 3. With the use of the values of the mobility calculated in this way and the measured resistivity, the total carrier density, as shown in Fig. 5, was derived from Eq. (3). These n-versus-T values were fitted very well to Eq. (13) with parameters $n(T=0)=1.98\times10^{18}/\text{cm}^3$ and $E_F=0.0026$ eV.

A final method that we consider for analyzing the magnetoresistance of the BDF is a modification of a formula derived by Noto and Tsuzuku, Eq. (8). For simplicity, since $\alpha_3\sim0.01$, we set $\alpha_3=0$. Equation (8) then becomes

$$\frac{\Delta\rho}{\rho_0}=\frac{\bar{\mu}^2H^2\cos^2\theta}{1+[(n_e-n_h)/(n_e+n_h)]^2\bar{\mu}^2H^2\cos^2\theta}\ . \tag{14}$$

The total conductivity for the BDF can be calculated from

$$\langle\sigma(H)\rangle=\frac{1}{2\pi}\int_0^{2\pi}\sigma(H,\theta)d\theta\ , \tag{15}$$

so that

$$\langle\sigma(H)\rangle=\sigma(0)\left[\left[\frac{n_e-n_h}{n_e+n_h}\right]^2+\frac{4n_en_h}{(n_e+n_h)^2}\frac{1}{(1+\bar{\mu}^2H^2)^{1/2}}\right]\ . \tag{16}$$

For ease of analysis, Eq. (16) may be recast into the following form:

$$\frac{\rho(H)}{\rho_0}=\frac{(1+\bar{\mu}^2H^2)^{1/2}}{1+[(n_e-n_h)/(n_e+n_h)]^2[(1+\bar{\mu}^2H^2)^{1/2}-1]}\ . \tag{17}$$

We note that in the low-field limit of $\bar{\mu}^2H^2\ll1$, Eq. (17) reduces to Eq. (6). Unfortunately, Eq. (17) cannot be recast into a form suitable for plotting as a straight line as exemplified by Eq. (9). While a nonlinear least-squares-fitting procedure could be followed, we have employed an alternative technique with good success. We have seen that for a fiber's geometry, it is a reasonable approximation to replace H^2 in Eq. (1) by $\frac{1}{2}H^2$ since

$$\langle H^2\rangle\rightarrow\langle H^2\cos^2\theta\rangle\sim\langle H^2\rangle\langle\cos^2\theta\rangle=\tfrac{1}{2}H^2\ .$$

We have then taken Noto's and Tsuzuku's formula [Eq. (9)] modified in this way to obtain

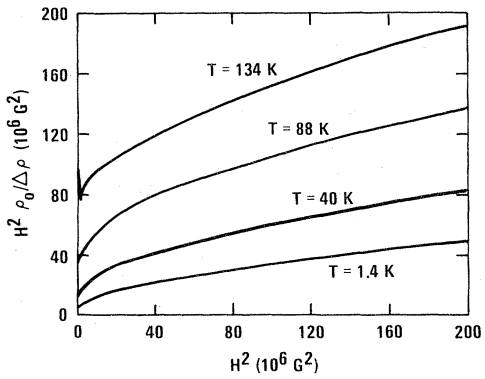

FIG. 6. $H^2/(\Delta\rho/\rho_0)$ vs H^2 for a variety of temperatures. Note the approximately linear dependence of the data on H^2 above a certain magnetic field H. The y intercept of the data yields the carrier mobility according to Eq. (18).

$$\frac{H^2}{\Delta\rho/\rho_0}=\frac{2}{\bar{\mu}^2}+\left[\frac{n_e-n_h}{n_e+n_h}\right]^2 H^2 . \tag{18}$$

Plotting the left-hand side of the equation versus H^2 should yield a straight line with y intercept $2(\bar{\mu})^{-2}$. As shown in Fig. 6, for a limited range of magnetic field the data do follow a straight line when plotted in this way, although significant deviations occur at low fields. Similar low-field behavior has been observed previously for pyrolytic and kish graphites and has been attributed to minority-carrier effects. The mobilities obtained from this analysis are displayed in Fig. 3 and are seen to be in good agreement with those values derived from the 3000-G data.

Using values of the mobility obtained via Eq. (18), we then attempted to fit Eq. (17) to the magnetoresistance data. The parameter $[(n_e-n_h)/(n_e+n_h)]^2$ was chosen by performing a visual best fit to the raw data. As shown in Fig. 1, excellent agreement was obtained over the entire magnetic field range sampled for all temperatures studied. This tends to lend credence to our graphical use of Eq. (18) to determine the carrier mobility, since the mobility more or less determines the slope of the $\Delta\rho/\rho_0$-versus-H curve and the slope of the fit is in close accord with the slope of the data.

With the use of the values of the mobility just derived in conjunction with the temperature-dependent resistivity values displayed in Fig. 4, the temperature dependence of the total carrier density $n=n_e+n_h$ was derived using Eq. (3) and is presented in Fig. 5. We again fitted the data using Eq. (13). As shown in Fig. 5, a good fit of the data to Eq. (13) was obtained using values of $E_F=0.0053$ eV, corresponding to a band overlap of 0.0106 eV, and

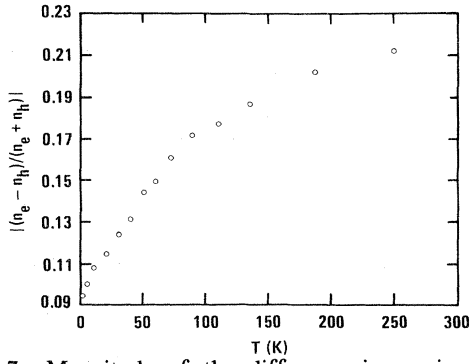

FIG. 7. Magnitude of the difference in carrier densities $|n_e-n_h|$ divided by the total carrier density $n=n_e+n_h$ vs temperature T derived by fitting the data of Fig. 1 to Eq. (17).

$n(T=0)=3.00\times10^{18}/\text{cm}^3$. The band overlap may be compared to a value of 0.03 eV derived from an analysis of galvanomagnetic de Haas–van Alphen oscillations for graphite single crystals at 4.2 K.[25] A summary of the carrier-density fits is presented in Table I.

The parameter $|(n_e-n_h)/(n_e+n_h)|$ derived in the above manner is plotted as a function of temperature in Fig. 7. The data exhibit a relatively smooth, monotonic dependence on the temperature. Using the variation of the total carrier density $n=n_e+n_h$ with temperature displayed in Fig. 5, we have also derived the temperature dependence of $|n_e-n_h|$ which is presented in Fig. 8. These data are in reasonable agreement with values of n_e-n_h quoted by Soule[18] [$n_e-n_h=0.4$ $(0.3)\times10^{18}/\text{cm}^3$ for his single-crystal graphite sample EP 14 (EP 7) at 4.2 K] and with those derived by Noto and Tsuzuku[20] ($n_e-n_h=0.8\times10^{18}/\text{cm}^3$ at 77 K for a pyrolytic-graphite sample heat-treated to 3600 °C).

As a final comment, we note that both Endo *et al.*[1] and Chieu *et al.*[2] have reported that there is an angular dependence to the transverse magnetoresistance of the BDF as it is rotated about its axis, a fact which Chieu *et al.*[2] have ascribed to the faceted structure of the annealed BDF. To strictly compare our magnetoresistance results with the theoretically derived expressions, which involve integrations over the angular dependence, we should have rotated our fiber about its axis and used the average value to compare with the theoretical expressions. However, the resultant angular variations in magnetoresistance for a BDF annealed at ~3000 °C are small: At 77 K in a field of 10 kG the variation is ~5% as the fiber is rotated by 180°,[1] while at 4.2 K and 15 T, the variation is ~10% as[2] the fiber is rotated through 90°. We have therefore not rotated our fibers and feel justified in comparing our experimental data with the theoretically derived expressions.

TABLE I. Electronic properties of a BDF annealed at 3000 °C.

Method	Description	μ_{BS} (10^4 cm²/V sec)	L_{BS} (μm)	$n(T=0)$ (10^{18}/cm³)	E_F (eV)
1	Low-field limit of Eq. (6)	8.79	1.32	1.09	0.002
2	Equation (7) using $H=3000$ G	4.15	0.62	2.31	0.004
3	Equation (7) using $\Delta\rho/\rho_0=0.5$	4.84	0.73	1.98	0.0026
4	Equation (17)	3.19	0.48	3.00	0.0053

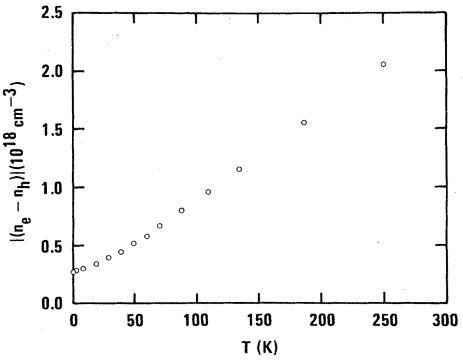

FIG. 8. Magnitude of the difference in carrier densities $|n_e - n_h|$ vs temperature T calculated using the data of Figs. 5 and 7.

V. DISCUSSION

We have presented a considerable body of magnetoresistance data taken at a variety of temperatures between 1.4 and 250 K. Our initial motivation in undertaking this study was to try to understand the magnetoresistance and to determine carrier mobilities. In the absence of Hall-effect measurements on the BDF, which would be difficult to perform and interpret, we have also attempted to derive carrier densities using both the magnetoresistance and resistivity data. Four different methods for analyzing the magnetoresistance data have been employed: Method 1, using the low-field data and Eq. (6); method 2, using the magnetoresistance at a single fixed field of $H=3000$ G and Eq. (7); method 3, using the magnetoresistance where $\Delta\rho/\rho_0=0.5$ and Eq. (7); and method 4, using the high-field magnetoresistance data in conjunction with Eq. (17). Equation (17), which was derived using the model of Noto and Tsuzuku,[20] but modified for the fiber's geometry, provided a good fit to the data over the entire magnetic field and temperature ranges studied.

The temperature dependence of the carrier mobilities derived using these four models is displayed in Fig. 3. With the use of Eq. (3), the temperature dependence of the total carrier density was inferred from the mobilities calculated using the methods above and the measured resistivity and is presented in Fig. 5. We believe that the parameters derived using methods 2–4 give the most reasonable values of mobilities and carrier densities because of the following arguments. First, the mobilities calculated using methods 2–4 are in good agreement with each other, while the mobility calculated using method 1 is considerably higher. Second, the temperature dependence of the resistivity of the BDF annealed at 3000 °C is very similar to that of the basal-plane resistivity of pyrolytic graphites annealed at 2750 and 3000 °C (see Fig. 5 of Ref. 16). In all of these cases, the resistivity increases very slightly with decreasing temperature from $\sim$300 down to $\sim$50 K, whereas below 50 K it drops considerably. In addition, the room-temperature resistivity of the BDF of $\rho(300\text{ K}) \sim 65\ \mu\Omega$ cm is greater than $\rho(300\text{ K})$ for a PG annealed at 3000 °C, but less than that of a PG annealed at 2750 °C. Thus, the resistivity data of the BDF annealed at 3000 °C indicate that its electronic properties are the same as that of a pyrolytic graphite annealed between 2750 and 3000 °C.

It is interesting to note, then, that the values of the mobilities derived using methods 2–4 lie in between the mobility values derived by Klein for PG's which have undergone heat-treatment temperatures T_{HT}'s of 2750 and 3000 °C (see Fig. 6 of Ref. 16). The low-temperature values of the mobility derived from method 1 lie above those of the PG sample annealed at 3000 °C, which can be used to argue that this method is not applicable for deriving the majority-carrier mobilities in the BDF. Another reason for not trusting method 1 is that it relies on $\Delta\rho/\rho_0$ strictly following an H^2 dependence at low fields at all temperatures studied, and our analysis of the data has shown that this is not true. Finally, as pointed out by Noto and Tsuzuku[20] and Kawamura *et al.*,[21] the low-field magnetoresistance can be considerably influenced by the presence of highly mobile minority carriers. In fact, the higher values of the mobilty derived using method 1 as compared to methods 2–4 suggest this.

The temperature dependence of the mobility derived using methods 2–4 is also in good agreement with those values derived by Klein[16] for the PG samples. Klein found that for a PG sample heat-treated at 2750 °C, $\mu(T)\sim T^{-0.63}$ between 77 and 300 K, while for a PG heat-treated to 3000 °C, $\mu(T)\sim T^{-0.86}$. In this temperature range, using method 2 we find $\mu(T)\sim T^{-0.64}$, while method 3 gives $\mu(T)\sim T^{-0.69}$ and method 4 yields $\mu(T)\sim T^{-0.51}$ for the BDF. These values are in close accord with those derived for the PG samples. While the slope of the μ-versus-T curve derived using method 1 changes considerably, taking only the 77 and 249-K values, then $\mu(T)\sim T^{-0.95}$ somewhat above the PG values. These values differ considerably from the slopes of the $\mu(T)$-versus-T curves in this temperature range for single-crystal graphite,[18] kish graphite,[21] and PG annealed at $\sim$3500 °C,[16,21,26,27] which varied from $T^{-1.0}$ to $T^{-1.6}$. Since the dependence of the mobility of carriers in the BDF on the temperature is considerably less than the temperature dependence of very-highly-ordered graphites and even less than the T^{-1} dependence expected from thermal phonon scattering, this suggests that defect-induced boundary scattering is still a major factor in determining the mobility of the BDF even near room temperature.

The carrier densities derived using methods 1–4 are displayed in Fig. 5. The $n(T)$ values derived using methods 2–4 are in fairly good agreement with each other and with the $n(T)$ values found by Klein for PG annealed at 2750 and 3000 °C (see Fig. 7 of Ref. 16), again supporting our assertion that the BDF annealed at 3000 °C behaves electronically like a PG annealed between 2750 and 3000 °C. The $n(T)$ values calculated from method 1 deviate significantly at low temperatures from those calculated with methods 2–4 and are significantly different from Klein's numbers. In addition, the STB model which successfully fitted $n(T)$ plots derived using methods 2–4, as well as Klein's data, was unable to reproduce the $n(T)$ plot inferred from method 1. This again supports our assertion that method 1 is not a satisfactory model for analyzing the electronic parameters of the BDF.

Using the values of carrier mobilities and carrier densi-

ties derived above, let us now reexamine the temperature dependence of the resistivity of the BDF. From room temperature down to ~ 50 K, the resistivity increases slightly. Although the mobility is increasing with decreasing temperature in this temperature range, the carrier density is decreasing faster than the mobility is increasing so that the resistivity increases. However, below 50 K, the carrier density is decreasing slower than the mobility is increasing so that the resistivity decreases with decreasing temperature.

Next, we will attempt to generalize our findings in order to understand in detail the temperature dependence of the mobility and the resistivity of the BDF and apply these considerations to the understanding of the general temperature dependence of the resistivity of graphites annealed at temperatures ranging from ~ 2500 °C to greater than ~ 3500 °C. Klein[16,26,28] has argued that the mobility of the carriers in graphite can be fitted very well by an equation of the form

$$\frac{1}{\mu(T)} = \frac{1}{\mu_{BS}} + \frac{1}{\mu_{ph}(T)} , \tag{19}$$

where $\mu(T)$ is the total mobility, μ_{BS} is the temperature-independent term due to boundary scattering, and $\mu_{ph}(T)$ is the temperature-dependent term arising from thermal phonon scattering. By varying only the temperature-independent μ_{BS} term, he was able to successfully fit the temperature dependence of the mobility for PG's annealed at a variety of temperatures. Klein[26] also found, using mobilities derived from magnetoresistance data and Eq. (3), that there are relatively small changes in the carrier density in a variety of PG specimens heat-treated at various temperatures greater than ~ 2500 °C.

A number of studies have addressed the behavior of the temperature dependence of the $\mu_{ph}(T)$ term. These investigations have yielded values ranging from $\mu_{ph}(T) \sim T^{-1.6}$ (Ref. 26) to $\mu_{ph}(T) \sim T^{-1.2}$ (Refs. 16, 18, and 21) to $\mu_{ph}(T) \sim T^{-1.0}$ (Ref. 27), the value expected from thermal phonon scattering. These values are all derived from data using single crystals or PG's annealed at ~ 3500 °C since, for these materials, the amount of boundary scattering is small (so that μ_{BS} is large) and the temperature dependence of the $\mu_{ph}(T)$ term can become evident at reasonable temperatures.

Using the above information, the mobility data derived using the modified Noto-Tsuzuku formula ("method 4") of Fig. 3 were fitted using Eq. (19). Various theoretical curves were investigated using $T^{-1.0}$, $T^{-1.2}$, and $T^{-1.6}$ dependences for the $\mu_{ph}(T)$ term in Eq. (19). The best fits shown in Fig. 9 correspond to (1) $\mu_{BS}=3.3\times10^4$ cm^2/V sec and $\mu_{ph}(T)=(3.4\times10^6)T^{-1.0}$ cm^2/V sec; (2) $\mu_{BS}=3.19\times10^4$ cm^2/V sec and $\mu_{ph}(T)=(1\times10^7)T^{-1.2}$ cm^2/V sec; and (3) $\mu_{BS}=3.19\times10^4$ cm^2/V sec and $\mu_{ph}(T)=(8\times10^7)T^{-1/6}$. Among the curves shown, the $T^{-1.0}$ fit achieves the best agreement with the data. Next, using the carrier density derived from "method 4" [Eq. (13) with $E_F=0.0053$ eV and $n(T=0)=3.0\times10^{18}$/cm^3] and the mobility curves generated from Eq. (19) with the parameters listed above, the resistivity curves presented in Fig. 4 were calculated from Eq. (3). Over the range 0 to 300 K, the data agree with the $T^{-1.0}$ fit to within 5%. The upward trend of the resistivity with decreasing temperature as well as the sharp drop of the resistivity below ~ 50 K are reproduced fairly successfully, suggesting that no novel mechanism need be invoked to explain the sharp drop of the resistivity. While the data below room temperature appear to be fitted best by the $T^{-1.0}$ dependence, the resistivity curve generated above room temperature with this dependence continues to decrease. In contrast, the data of Chieu *et al.*[14] on a BDF annealed at 2900 °C exhibit a positive temperature coefficient of resistivity above ~ 300 K. Their data are qualitatively similar to the resistivity curve generated using the $T^{-1.2}$ dependence for $\mu_{ph}(T)$ over the entire temperature range explored—up to 1100 K.

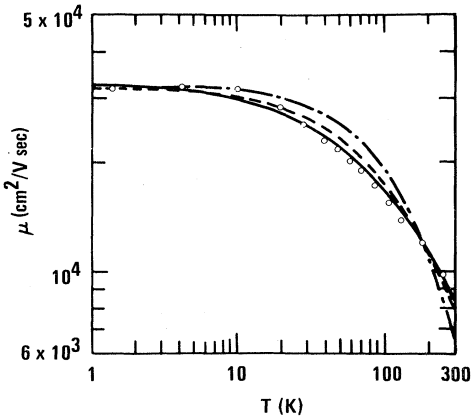

FIG. 9. Mobility μ vs temperature T derived using the modified Noto-Tsuzuku formula, Eq. (17). Shown are best fits of the data to Eq. (19) using (1) $\mu_{BS}=3.3\times10^4$ cm^2/V sec and $\mu_{ph}(T)=(3.4\times10^6)T^{-1.0}$ cm^2/V sec (solid curve); (2) $\mu_{BS}=3.19\times10^4$ cm^2/V sec and $\mu_{ph}(T)=(1\times10^7)T^{-1.2}$ cm^2/V sec (dashed curve); and (3) $\mu_{BS}=3.19\times10^4$ cm^2/V sec and $\mu_{ph}(T)=(8\times10^7)T^{-1.6}$ cm^2/V sec (long-dashed—short-dashed curve).

As we have noted above, Klein[26] has argued that past a certain graphitization stage that occurs at ~ 2500 °C, the carrier density is no longer seriously affected by increases in the heat-treatment temperature. Therefore we will assume that the temperature-dependent carrier density is independent of heat-treatment temperature in the analysis below and is given by Eq. (13) with $E_F=0.0053$ eV and $n(T=0)=3.0\times10^{18}$/cm^3. Next, we assume that the mobility obeys the form of Eq. (19) with $\mu_{ph}(T)=(3.4\times10^6)T^{-1.0}$ cm^2/V sec. It is reasonable to assume, as Klein has done previously,[26] that varying the heat-treatment temperature above ~ 2500° essentially only affects the crystallite size and hence the boundary scattering term μ_{BS}. Chieu *et al.*[2] have also pointed out that the large difference in the magnitude of the magnetoresistance of various types of graphite reflects differences in crystalline perfection. We have therefore generated a variety of resistivity curves using Eq. (3) where the only parameter changed has been the μ_{BS} term. As presented in Fig. 10, by only varying the crystallite size through the variable μ_{BS}, Klein's temperature dependence of the basal-plane resistivity curves of PG's heat-treated between 2500 and 3000 °C (see Fig. 5 of Ref. 16) can be accurately reproduced. We can also reproduce the temperature depen-

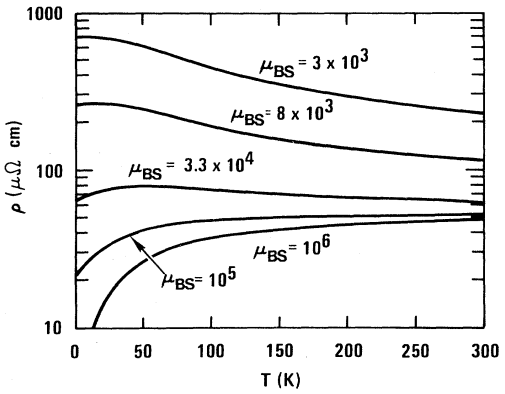

FIG. 10. Resistivity ρ vs temperature T. These curves were derived using Eq. (3) where n is given by Eq. (13) with $E_F=0.0053$ eV and $n(T=0)=3.0\times10^{18}/\text{cm}^3$ and μ is given by Eq. (19) with $\mu_{\text{ph}}(T)=(3.4\times10^6)T^{-1.0}$ cm^2/V sec. Varying only the parameter μ_{BS}, which is determined by the amount of boundary scattering (i.e., the size of the crystallites), generates these curves which faithfully reproduce the resistivity curves for pyrolytic graphites and benzene-derived graphite fibers annealed at temperatures between $\sim$2500 and $\sim$3500 °C.

dence of the electrical resistivity of the BDF annealed at temperatures between 2500 and 3500 °C as presented in Fig. 7 of Ref. 2 and Fig. 1 of Ref. 29. Thus, this simple model seems to provide an accurate description of the electronic properties of annealed pyrolytic graphites and graphite fibers.

The $T=0$ value of the mobility, $\bar{\mu}(T=0)=\mu_{\text{BS}}$, can also be used to estimate the boundary-limited mean free path L_{BS}. Klein[26] has used the formula

$$L_{\text{BS}}=\frac{m^*v\bar{\mu}(T=0)}{e\times10^7}\ , \tag{20}$$

where $m^*v=(2.4\pm0.8)\times10^{-21}$ g cm sec^{-1} to calculate L_{BS} from μ_{BS}. Using values of the mobility generated using methods 1–4, the corresponding L_{BS} values were calculated using Eq. (20) and are shown in Table I. In accord with the discussion above, the values calculated from methods 2–4 are in good agreement and a typical value of L_{BS} appears to be 0.5 μm for the BDF annealed at 3000 °C. The ρ-versus-T data for a BDF annealed at 2500 and 2800 °C of Ohhashi *et al.*[29] can also be analyzed. Their data indicate $\rho(T=0)\sim70\ \mu\Omega$ cm for $T_{\text{HT}}=2800$ °C and $\rho(T=0)\sim270\ \mu\Omega$ cm for $T_{\text{HT}}=2500$ °C. From the analysis above, we estimate $\mu_{\text{BS}}=3\times10^4$ cm^{2}V sec for $T_{\text{HT}}=2800$ °C and $\mu_{\text{BS}}=8\times10^3$ cm^2/V sec for $T_{\text{HT}}=2500$ °C. In conjunction with Eq. (20), these values imply $L_{\text{BS}}\sim0.45$ μm for $T_{\text{HT}}=2800$ °C and $L_{\text{BS}}\sim0.12$ μm for $T_{\text{HT}}=2500$ °C, which may be compared with the crystallite size estimated from x-ray diffraction,[29] ~0.1 μm for a T_{HT} of 2800 °C and ~0.06 μm for a T_{HT} of 2500 °C. The agreement is rather good in view of the simple models used. We should also note that for a BDF annealed at 3500 °C,[2] $\rho(T=0)\sim22\ \mu\Omega$ cm, implying that $\mu_{\text{BS}}\sim10^5$ cm^2/V sec. From Eq. (20), this suggests that $L_{\text{BS}}=1.5$ μm is the largest typical crystallite size that can be obtained in the BDF.

VI. CONCLUSIONS

In conclusion, we have performed detailed magnetoresistance measurements at a variety of temperatures on a benzene-derived graphite fiber annealed at 3000 °C. Four ways of inferring the carrier mobility from the magnetoresistance data were employed, three of which were based on Eq. (7), while one was derived using the model of Noto and Tsuzuku.[20] A modification of this model, Eq. (17), was found to accurately fit the magnetoresistance data at a variety of temperatures over the entire magnetic field range studied. The temperature dependence of the carrier mobility data derived using Eq. (17) was fitted using Eq. (19), which consists of a temperature-dependent term arising from thermal phonon scattering [$\mu_{\text{ph}}(T)=(3.4\times10^6)T^{-1.0}$ cm^2/V sec] and a temperature-independent term arising from boundary scattering ($\mu_{\text{BS}}=3.3\times10^4$ cm^2/V sec). With the use of mobility data derived from Eq. (17) in conjunction with the measured resistivity, values of the carrier density were calculated via Eq. (3). The temperature dependence of the carrier density obeyed Eq. (13) with $n(T=0)=3\times10^{18}/\text{cm}^3$ and $E_F=0.0053$ eV. Assuming that the temperature-dependent carrier density and the thermal-phonon-induced mobility remain constant with increasing heat-treatment temperature, the temperature dependence of the resistivity of PG's and BDF's annealed at temperatures between $\sim$2500 and $\sim$3500 °C could be quantitatively reproduced by varying the amount of temperature-independent boundary scattering μ_{BS} which is related to the crystallite size.

ACKNOWLEDGMENTS

We would like to thank Professor M. S. Dresselhaus, Dr. J. Howe, Dr. B. W. McQuillan, Dr. R. B. Olsen, Dr. R. L. Freeman, and Professor L. J. Sham, for enlightening conversations.

[1]M. Endo, Y. Hishiyama, and T. Koyama, J. Phys. D **15**, 353 (1982).
[2]T. C. Chieu, G. Timp, M. S. Dresselhaus, M. Endo, and A. W. Moore, Phys. Rev. B **27**, 3686 (1983).
[3]T. Koyama, M. Endo, and T. Onuma, Jpn. J. Appl. Phys. **11**, 445 (1972).
[4]T. Koyama, Carbon **10**, 757 (1972).
[5]T. Koyama and M. Endo, Jpn. J. Appl. Phys. **13**, 1175 (1974).
[6]T. Koyama, M. Endo, and Y. Hishiyama, Jpn. J. Appl. Phys. **13**, 1933 (1974).
[7]A. Oberlin, M. Endo, and T. Koyama, J. Cryst. Growth **32**, 335 (1976).
[8]M. Endo, A. Oberlin, and T. Koyama, Jpn. J. Appl. Phys. **16**, 1519 (1977).
[9]M. Endo, T. Koyama, and Y. Hishiyama, Jpn. J. Appl. Phys. **15**, 2073 (1976).

[10]A. Oberlin, M. Endo, and T. Koyama, Carbon **14**, 133 (1976).
[11]M. Endo, T. Koyama, and M. Inagaki, Synth. Metals, **3**, 177 (1981).
[12]G. P. Davis, M. Endo, and F. L. Vogel, in *Extended Abstracts of the 15th Biennial Conference on Carbon, Philadelphia, Pennsylvania, 1981,* edited by W. C. Forsman (American Carbon Society, University Park, PA, 1981), p. 363.
[13]T. C. Chieu, M. S. Dresselhaus, and M. Endo, Phys. Rev. B **26**, 5867 (1982).
[14]T. C. Chieu, M. S. Dresselhaus, and M. Endo, in *Extended Abstracts of the 16th Biennial Conference on Carbon, July 18—22, 1983, San Diego, California,* edited by G. B. Engle (American Carbon Society, University Park, PA, 1983), p. 272.
[15]M. Endo, T. C. Chieu, G. Timp, and M. S. Dresselhaus, in *Extended Abstracts of the 16th Biennial Conference on Carbon, July 18—22, San Diego, California,* Ref. 14, p. 219.
[16]C. A. Klein, J. Appl. Phys. **33**, 3338 (1962).
[17]C. A. Klein and W. D. Straub, Phys. Rev. **123**, 1581 (1961).
[18]D. E. Soule, Phys. Rev. **112**, 698 (1958).
[19]J. W. McClure, Phys. Rev. **112**, 715 (1958).
[20]K. Noto and T. Tsuzuku, Jpn. J. Appl. Phys. **14**, 46 (1975).
[21]K. Kawamura, T. Saito, and T. Tsuzuku, J. Phys. Soc. Jpn. **42**, 574 (1977).
[22]T. Tsuzuku, Carbon **21**, 415 (1983).
[23]R. O. Dillon, I. L. Spain, J. A. Woollam, and W. H. Lowrey, J. Phys. Chem. Solids **39**, 907 (1978).
[24]I. L. Spain, in *Chemistry and Physics of Carbon,* edited by P. L. Walker and P. A. Thrower (Dekker, New York, 1973), Vol. 8, p. 104.
[25]D. E. Soule, Phys. Rev. **112**, 708 (1958).
[26]C. A. Klein, J. Appl. Phys. **35**, 2947 (1964).
[27]C. A. Klein, W. D. Straub, and R. J. Diefendorf, Phys. Rev. **125**, 468 (1962).
[28]C. A. Klein, Rev. Mod. Phys. **34**, 56 (1962).
[29]K. Ohhashi, J. Amiell, P. Delhaes, J. F. Mareche, D. Guerard, and M. Endo, in *Extended Abstracts of the 16th Biennial Conference on Carbon, July 18—22, 1983, San Diego, California,* Ref. 14, p. 271.